Linear disturbances shift boreal peatland plant communities toward earlier peak greenness

Scott J. Davidson[1], Ellie M. Goud[1], Avni Malhotra[2], Claire O. Estey[1], Percy Korsah[1], and Maria Strack[1]

[1]University of Waterloo
[2]Stanford University

November 26, 2022

Abstract

Vast areas of boreal peatlands are impacted by linear disturbances known as seismic lines. Tree removal and ground disturbance alter vegetation communities and are expected to change ecosystem functioning. We investigate seismic line disturbances on peatland plant community composition and phenological patterns using readily available digital photography at a bog and a fen in Alberta, Canada. Our objectives were to: 1) compare the understory vegetation on seismic lines with those in adjacent undisturbed peatlands using two phenological metrics (green and red chromatic coordinates); 2) evaluate if vegetation greenness is directly related to vegetation community composition, and 3) determine whether plot-scale greenness predicts plant productivity. We found that disturbed peatlands have an earlier seasonal peak (maximum greenness) compared to undisturbed areas, and vegetation communities had a stronger relationship to greenness and gross primary production (GPP) at disturbed sites relative to undisturbed sites. This change in understory vegetation results in greater CO_2 uptake in disturbed sites. We demonstrate an easy-to-use application of digital photography that successfully quantifies phenological changes in boreal peatland vegetation. This non-destructive method for understanding vegetation phenology eliminated the need for fixed infrastructure and allowed us to sample more plots and study sites while allowing for repeated measures in the future. As boreal landscapes continue to be disturbed by linear disturbances, understanding the magnitude and mechanisms of vegetation and phenology changes is the first step toward predicting carbon cycling changes across broad spatial scales.

1

Linear disturbances shift boreal peatland plant communities toward earlier peak greenness

Scott J. Davidson[1*], Ellie M. Goud[1], Avni Malhotra[2], Claire O. Estey[1], Percy Korsah[1] and Maria Strack[1]

[1] Department of Geography and Environmental Management, University of Waterloo, Waterloo, ON, Canada, N2L 3G1

[2] Department of Earth System Science, Stanford University, Stanford, CA, USA 94305

Corresponding author: Scott J. Davidson (s7davidson@uwaterloo.ca)

Key Points:

- Linear disturbances cause a shift in vegetation communities and changes in green leaf phenology and greenness metrics.
- Readily available smartphone photography successfully captured the phenological characteristics of these vegetation types.
- The change in vegetation causes greater CO_2 uptake in the disturbed sites and greenness metrics were good predictors of these CO_2 changes.

18 **Abstract**

19 Vast areas of boreal peatlands are impacted by linear disturbances known as seismic lines. Tree
20 removal and ground disturbance alter vegetation communities and are expected to change
21 ecosystem functioning. We investigate seismic line disturbances on peatland plant community
22 composition and phenological patterns using readily available digital photography at a bog and a
23 fen in Alberta, Canada. Our objectives were to: 1) compare the understory vegetation on seismic
24 lines with those in adjacent undisturbed peatlands using two phenological metrics (green and red
25 chromatic coordinates); 2) evaluate if vegetation greenness is directly related to vegetation
26 community composition, and 3) determine whether plot-scale greenness predicts plant
27 productivity. We found that disturbed peatlands have an earlier seasonal peak (maximum
28 greenness) compared to undisturbed areas, and vegetation communities had a stronger
29 relationship to greenness and gross primary production (GPP) at disturbed sites relative to
30 undisturbed sites. This change in understory vegetation results in greater CO_2 uptake in disturbed
31 sites. We demonstrate an easy-to-use application of digital photography that successfully
32 quantifies phenological changes in boreal peatland vegetation. This non-destructive method for
33 understanding vegetation phenology eliminated the need for fixed infrastructure and allowed us
34 to sample more plots and study sites while allowing for repeated measures in the future. As
35 boreal landscapes continue to be disturbed by linear disturbances, understanding the magnitude
36 and mechanisms of vegetation and phenology changes is the first step toward predicting carbon
37 cycling changes across broad spatial scales.

38 **Plain Language Summary**

39 Industrial activities for oil and gas mining across boreal North America can result in a vast
40 network of linear disturbances called seismic lines. These are narrow clearings cut across
41 peatlands and forests, resulting in the removal of trees and compaction to the soil, leading to
42 changes in how these ecosystems function. One such impact is on how the ground-layer
43 vegetation communities green up over the course of the growing season and how this impacts
44 how productive they are. In this study we investigated the greenness patterns of vegetation
45 communities at two different peatland types impacted by seismic lines. To do this, we collect
46 photographs using smartphones, alongside vegetation surveys and carbon exchange
47 measurements. We found that these disturbances significantly impact the greenness of these
48 communities, with disturbed sites becoming more productive faster. Using smartphones to
49 collect photographs provided a quick and easy method to collect greenness data without the need
50 for expensive equipment or fixed infrastructure. As boreal peatlands continue to be under threat
51 from increased disturbances, this study provides a first step in understanding how their greenness
52 and productivity may change in the future.

53

54 **1. Introduction**

55   Peatlands cover 25 – 30 % of the boreal zone and are important component of both
56 regional and global carbon cycle dynamics (Wieder et al., 2006). However, industrial activities
57 for resource extraction in these areas have led to an extensive network of linear disturbances
58 known as seismic lines. In fact, there are an estimated 345,000 km (disturbing an area of ~1900
59 km^2) of seismic lines crossing peatlands in the province of Alberta, Canada alone (Strack et al.,
60 2019). These linear clearings can be between 1.5 and 10 m wide, creating a dense grid across the

61 landscape and are cleared using a combination of tree removal and soil disturbance/compaction
62 altering hydrological conditions (Braverman & Quinton, 2016), vegetation communities
63 (Echiverri et al., 2020) and ecosystem functions such as carbon exchange (Dabros et al., 2018;
64 Davidson et al., 2020).

65   Given the geographic extent and impact of seismic lines, there is a push to restore them in
66 order to return habitat quality and ecosystem function (Filicetti et al., 2019). Current restoration
67 methods, however, are based on forestry practices developed for upland, drier ecosystems and
68 may not translate to wetlands (Davidson et al., 2020). Restoration of seismic lines often involves
69 a technique called mounding, used to bring back localised microtopography necessary for tree
70 regeneration (Pyper et al., 2014). Yet, this method may be detrimental to the existing vegetation
71 communities in peatlands, especially given that, although there is a shift in vegetation
72 community on seismic lines, the species present are still peat forming and therefore important to
73 the overall carbon balance (Echiverri et al., 2020). Furthermore, the disturbance caused by these
74 mounding techniques has been shown to potentially increase decomposition and carbon loss
75 from soils (Davidson et al., 2020). A greater understanding of peatland vegetation communities
76 present post-disturbance is imperative for improving restoration best practices. Given the extent
77 of the disturbed area, it would also be beneficial to develop techniques that capture plot-scale
78 vegetation change and carbon dynamics that do not rely on fixed infrastructure.

79   Phenology is used to describe the development of plant properties related to temporal
80 variation in life history events (e.g., flowering time, bud break, leaf senescence) (White et al.,
81 1997). The phenology of leaf traits (e.g., greenness, timing of leaf-out and senescence) are
82 important drivers of terrestrial carbon cycling (Hufkens et al., 2012). High quality measurements
83 of green leaf phenology (hereafter referred to as phenology) are integral in understanding the
84 effects of environmental change on ecosystem function and biosphere-atmosphere interactions
85 (Hufkens et al., 2012). In peatlands, vegetation phenology is linked to abiotic drivers such as
86 temperature, water, and nutrient availability (Bubier et al., 2006), is often the first to respond to
87 environmental change (Richardson et al., 2018; Malhotra et al., 2020) and has downstream
88 influences on ecosystem function such as increased ecosystem carbon losses (Hanson et al.,
89 2020). A multitude of non-destructive vegetation assessments (Lavorel & Garnier 2002; Goud et
90 al., 2017; Girard et al., 2020) and site-scale phenology-function investigations (Wilson et al.,
91 2008; Goud et al., 2017) exist. However, evaluation of seismic line disturbance effects on
92 peatlands requires a combination of non-destructive vegetation measurements and phenology-
93 function link investigations that can be rapidly implemented across multiple sites and that can be
94 revisited over multiple years.

95   Red-Blue-Green (RGB) photography is one such non-destructive method that may be
96 useful in understanding plant phenological characteristics. Land-surface phenology studies
97 typically use remote sensing products, which inform large-scale phenological patterns. However
98 given the highly heterogeneous nature of peatland ecosystems, RGB photography using hand-
99 held cameras enables plot-scale studies that may provide valuable information that is lost at
100 larger scales (Linkosalmi et al., 2016) and could also allow for a greater understanding of
101 ecosystem carbon flux dynamics with very little interaction with the vegetation itself. RGB
102 photographs can be used to calculate greenness indices such as the green chromatic coordinate
103 (*Gcc*), which indicates vegetation greenness or 'health' across a number of ecosystem types
104 (Sonnentag et al., 2012). Phenological characteristics can also be used to distinguish between
105 different plant communities (e.g., Wu et al., 2021). Although greenness at one point in time

106 might not be a useful metric, the phenological pattern will vary between species and/or
107 functional groups. RGB photographs can also be used to calculate other indices such as the red
108 chromatic coordinate (*Rcc*). *Rcc* has been successfully used to monitor vegetation senescence
109 (Liu et al., 2020) and investigate plant stress after water table drawdown (Peichl et al., 2015).
110 The difference in reflectance in the red spectrum could also allow for separation among common
111 peatland plant functional groups, namely vascular versus non-vascular plants, that have different
112 impacts on ecosystem function (e.g., rates of nutrient cycling, carbon storage; Zeh et al., 2020).

113 The creation of seismic line disturbances is expected to influence peatland plant
114 communities, phenological characteristics and carbon exchange, however studies on this are
115 lacking. Strack et al. (2018) found a significant increase in graminoid cover linked to a shift in
116 hydrological conditions on a winter road (a similar, fully vegetated, linear disturbance type)
117 crossing a boreal peatland. This shift towards a more productive vegetation community resulted
118 in disturbed plots acting as a greater CO_2 sink but larger methane (CH_4) source compared to
119 adjacent peatland. Linked to this shift in vegetation community, is the reduced likelihood for tree
120 sapling regeneration due to them being outcompeted by more productive understory vegetation
121 such as sedges (Filicetti & Nielsen, 2020). Changes in plant species composition are likely to
122 influence phenological characteristics, with cleared areas following disturbance potentially
123 greening up faster due to an increase in solar radiation.

124 Phenological modelling of areas disturbed due to seismic lines is potentially a useful tool
125 for both disturbance evaluation on peatland carbon exchange and future variations under a
126 changing climate. Therefore, the objectives of this study were to: 1) evaluate differences in
127 vegetation communities found on seismic lines and those in the adjacent undisturbed forested
128 area using two phenological metrics, 2) evaluate if differences in greenness are related to
129 vegetation composition and 3) determine whether plot-scale greenness is a strong predictor of
130 CO_2 uptake (gross primary production; GPP). We hypothesized that plots on seismic lines would
131 green up earlier and be overall greener than those in undisturbed areas, resulting in greater CO_2
132 uptake during the summer period.

133

134 **2. Materials and Methods**

135 *2.1 Study sites and Experimental Design*

136 We sampled two boreal peatland sites in northern Alberta, Canada (Figure 1A-C)
137 between May and August 2019. Carmon Creek (hereafter referred to as bog; Figure 1D) is a
138 treed bog approximately 40 km northeast of Peace River, Alberta (56°21′44″ N, 116°47′45″W).
139 The seismic lines at Carmon Creek were created approximately 5-15 years ago and are
140 approximately 3 m wide. The second site IPAD (hereafter referred to as fen; Figure 1E) is a treed
141 poor fen located approximately 40 km northeast of Peace River (56°23′51.22″ N,
142 116°53'27.60″W). The seismic lines here were created approximately 20 years ago and are
143 approximately 7 m wide. Disturbed locations (on the seismic lines) at both sites are without tree
144 cover following disturbance. The 30 year (1981-2010) mean annual air temperature and annual
145 total precipitation are + 1.6 ° C and 386.3 mm respectively (mean May-August air temperature
146 and total precipitation are + 13.8 ° C and 213 mm; Environment Canada, 2019).
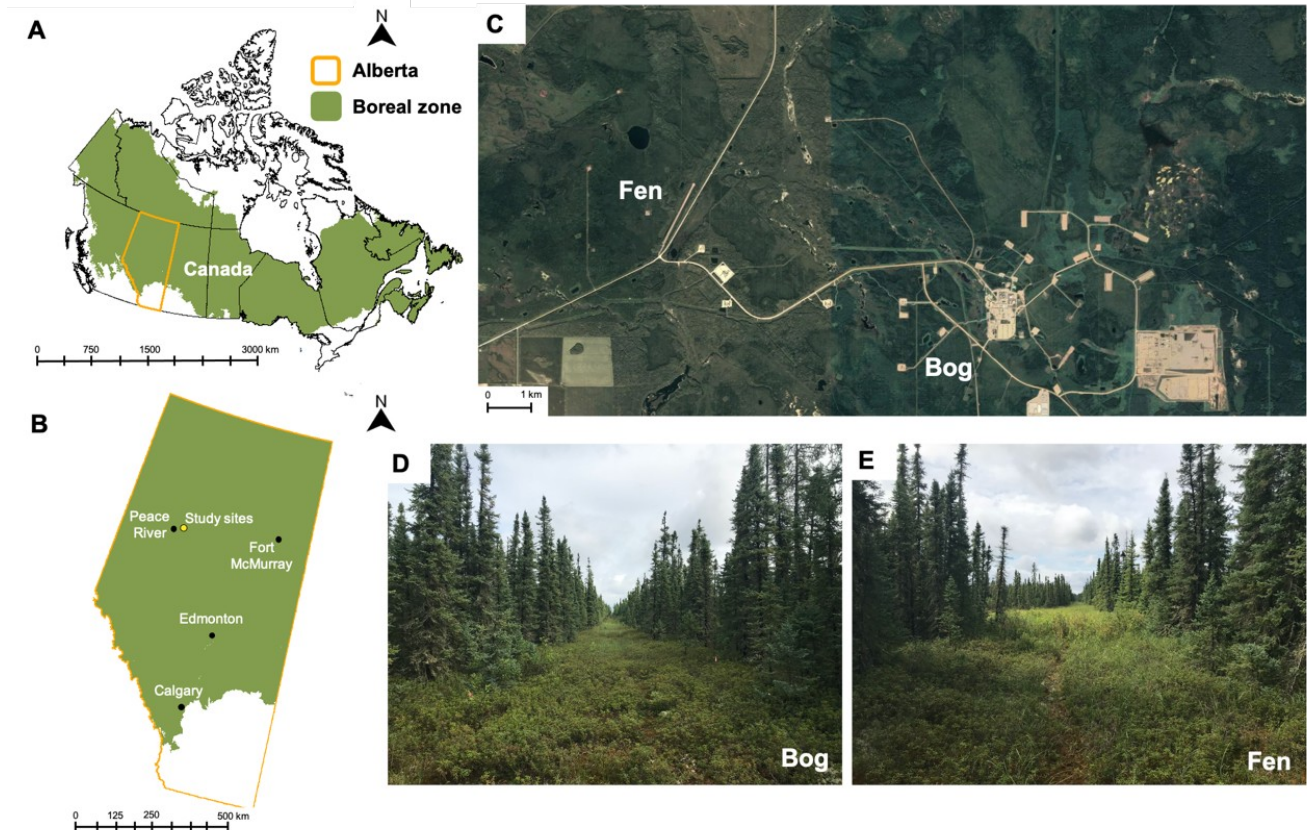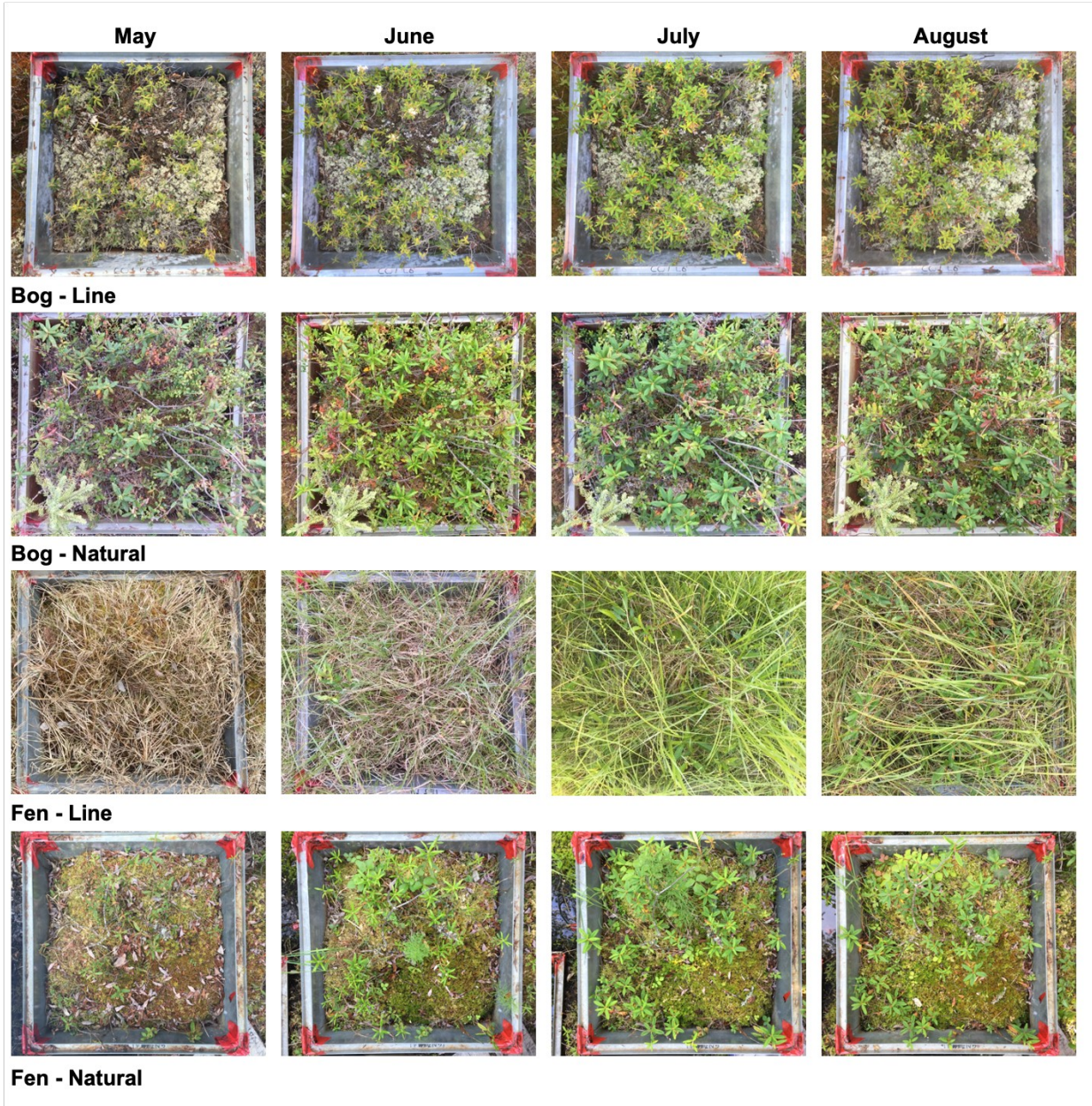
147

Figure 1. a) The location of the boreal zone (NRCan North American boreal zone layer; Brandt, 2009) and Alberta
within Canada. b) The location of the study sites within Alberta, c) The location of the two study areas (bog:
56°21′44″ N, 116°47′45″W and fen: 56°23′51.22″ N, 116°53'27.60″W) (base map: Google Earth: TerraMetrics
(Accessed February 9th, 2021) and photographs of the seismic line cutting across the d) bog and E) fen study sites.

In May 2018, 36 square plots (60 x 60 cm) were established for image, vegetation, and
gas flux measurements. Grooved aluminum collars were permanently installed to allow for
repeated measurements in the same location, located adjacent to boardwalks to minimize
disturbance to the peat and vegetation. Plots were established at three positions on a seismic line
in the dominant vegetation community present, and three in the adjacent undisturbed area at two
lines at the fen site (12 plots) and four lines at the bog site (24 plots).

2.2 Image collection and processing

Between 10 and 12 photographs were collected for each plot at each site between 12th
May and 22nd August 2019 (Figure 2) using a smartphone (iPhone 6, Apple, USA). All 420
photographs were captured under clear-sky or as near to clear-sky conditions as possible and
between 10:00 and 13:00. A marker was placed on the boardwalk at each plot to ensure
placement of the smartphone was approximately 1 m above the top of the ground layer canopy
and in the same position each time. The image acquisition mode was set to auto white balance
and autofocus. Photographs were stored in the joint photographic expert group (JPEG) format at
a resolution of 1334 x 750 dpi. Any photos with standing water were removed from the analysis

168 (five photos across two collars in total) to avoid backscatter skewing the calculated greenness
169 values.

170

171 **Figure 2.** Example photographs of plots at each peatland type and location (where line indicates that the plot was on
172 a seismic line and natural was the undisturbed plot) for each month of study indicating both the difference in
173 vegetation community and visual change in 'greenness' over the growing season

174   We used the R package 'Phenopix' version 2.3.1 (Filippa et al., 2016) to calculate the
175 green chromatic coordinate; *Gcc;*

176
$$Gcc = \frac{G_{DN}}{R_{DN+¿G_{DN+¿B_{DN}}}¿¿}$$
(1)

177 Where R_{DN}, G_{DN} and B_{DN} are the average red, green and blue digital numbers. *Gcc* was
178 chosen as it is generally more effective than other indices in minimizing the effects of scene
179 illumination (Sonnentag et al., 2012), which is particularly useful when using hand-held
180 equipment.

181 We also calculated the red chromatic coordinate; *Rcc;*

182
$$Rcc = \frac{R_{DN}}{R_{DN+\dot{c}G_{DN+\dot{c}B_{DN}}} \dot{c}\dot{c}}$$
(2)

183 We used the *DrawROI* function to delineate the Region-Of-Interest (ROI) for each plot
184 within the boundaries of the flux collar. We then used the *ExtractVIs* function to calculate the
185 chromatic coordinate indices on a per-pixel basis (Toomey et al. 2015).

186

2.3 Modelling seasonal greenness

188 To compare the seasonal trajectory of *Gcc* in a standardized way across our plots, while
189 accounting for missing measurements, we fit a Gaussian model to our *Gcc* values by day of year
190 (DOY) following Malhotra et al. (2015). We used the following model:

191
$$Gcc = a \times e^{-0.5\left[\frac{DOY-b}{c}\right]^2}$$
(3)

192 Where a, b and c are parameters describing the seasonal trajectory of *Gcc*: the peak value
193 of *Gcc* (a), the critical point i.e., DOY at peak *Gcc* (b) and the growth rate of the curve (c). These
194 parameters allows us to compare the peak, timing of peak and progression of phenology across
195 our plots. We generated this Gaussian model each for our 36 plots (Figure S1/S2) and analyzed
196 the three model parameters across bog/fen and line/natural site types. The majority of our
197 Gaussian model fit R^2 values were above 0.8 (22 plots), some between 0.7 and 0.8 (9 plots),
198 between 0.7 and 0.5 (3 plots) and below 0.5 (2 plots).

199

2.4 Plant species composition

201 Plant species composition within each plot was surveyed in July 2018. Percentage cover
202 of all vascular and non-vascular plant species were visually estimated and recorded as 0.1
203 (present), 1 (occasional, few individuals) or 3 (occasional, more individuals), and then rounded
204 up to the nearest 5%. All individuals were identified to species level, with species nomenclature
205 following the USDA online plants database (http://plants.usda.gov).

206

2.5 Gross primary production (GPP)

208 Carbon dioxide (CO_2) exchange was determined using the closed dynamic chamber
209 method (Alm et al. 2007). A clear acrylic chamber ($60 \times 60 \times 30$ cm) was placed on a stainless-
210 steel collar (60×60 cm). A groove in the collar was filled with water to create a seal when the
211 chamber was placed. A battery-operated fan circulated the headspace air throughout the
212 measurement period and the chamber was removed from the collar between each measurement
213 to equilibrate back to ambient CO_2 concentration and temperature. The concentration of CO_2
214 (ppm) was determined inside the chamber at 15 second intervals for a maximum of 2.5 minutes

215 using a portable infrared gas analyser (EGM-4, PP systems, Massachusetts, USA). The linear
216 change in CO_2 concentration over time was used to calculate net ecosystem exchange (NEE; g
217 CO_2 m^2 d^{-1}). Ecosystem respiration (ER; g CO_2 m^2 d^{-1}) was determined by darkening the chamber
218 with an opaque cloth shroud. Gross primary production (GPP; g CO_2 m^2 d^{-1}) was calculated as
219 the difference between NEE and ER. We express GPP as positive, indicating CO_2 uptake.

220 *2.6 Statistical analysis*

221   All analyses were performed in R3.5.3 (R Core Team 2019). We used two-way analysis
222 of variance (ANOVA) to look at the difference in *Gcc* and *Rcc* between on and off-line positions
223 across both sites. We performed correspondence analysis (CA) using the 'cca' function in the
224 'vegan' R package (Oksanen et al., 2019) to assess variation in plant species composition among
225 sites. CA maximizes between-group variance, assumes unimodal species responses along
226 environmental gradients, and is suitable for data matrices that contain many zero values
227 (Legendre & Legendre, 2012). We applied a Hellinger transformation on the percent cover data
228 matrix prior to CA analysis because of its ability to reduce asymmetry while being insensitive to
229 double zeroes. Linear regression was used to look at the relationship between maximum *Gcc* and
230 *Rcc* and the output of the correspondence analysis. An analysis of covariance (ANCOVA) was
231 used to look at the relationship between *Gcc* and GPP between plots on the seismic lines and in
232 the natural, undisturbed areas at both sites. Finally, a multiple regression model was used to look
233 at the relationship between both *Gcc* and *Rcc* on GPP at both peatland types and locations. All
234 statistics were performed on measured *Gcc* and not modelled *Gcc*. The modeled parameters were
235 primarily reported for a descriptive comparison of the seasonal peak timing (Table 1).

236

237 **3**. **Results**

238 *3.1 Plot level phenology metrics*

239   At the bog site, the plots on the seismic line were consistently greener over the course of
240 the growing season in comparison to the plots off-line in the adjacent natural area (Figure 3a).
241 By the end of August, both the disturbed and natural sites saw a dip in *Gcc*, likely linked to the
242 beginning of the senescence period. Unfortunately, due to logistical limitations, we were unable
243 to obtain photographs for the autumn period. At the fen site, the natural plots were greener in the
244 spring, but the on-line plots quickly caught up and by the end of the growing season both areas
245 had similar greenness levels (Figure 3a). Overall, greenness was significantly lower at the bog
246 compared to the fen (ANOVA; $F_{1,403} = 19.8$, $p < 0.001$). Yet, no significant difference in
247 greenness was found between on and off-line across both sites (ANOVA; $F_{1,403} = 0.2$, $p = 0.7$). In
248 comparison to the bog site, both locations at the fen site saw less of a decrease in *Gcc* at the end
249 of the growing season, likely due to the composition of the vegetation community present.

250   We also compared plot-scale modelled parameters of *Gcc* seasonal trajectory (Equation
251 3) across bog/fen and line/natural sites (Figure 3c, Table 1). At both the bog and fen, the line
252 plots had an earlier seasonal peak (maximum greenness) compared to natural areas. At the bog,
253 on average, the seasonal peak of *Gcc* was 7 days earlier on the line than in natural areas. At the
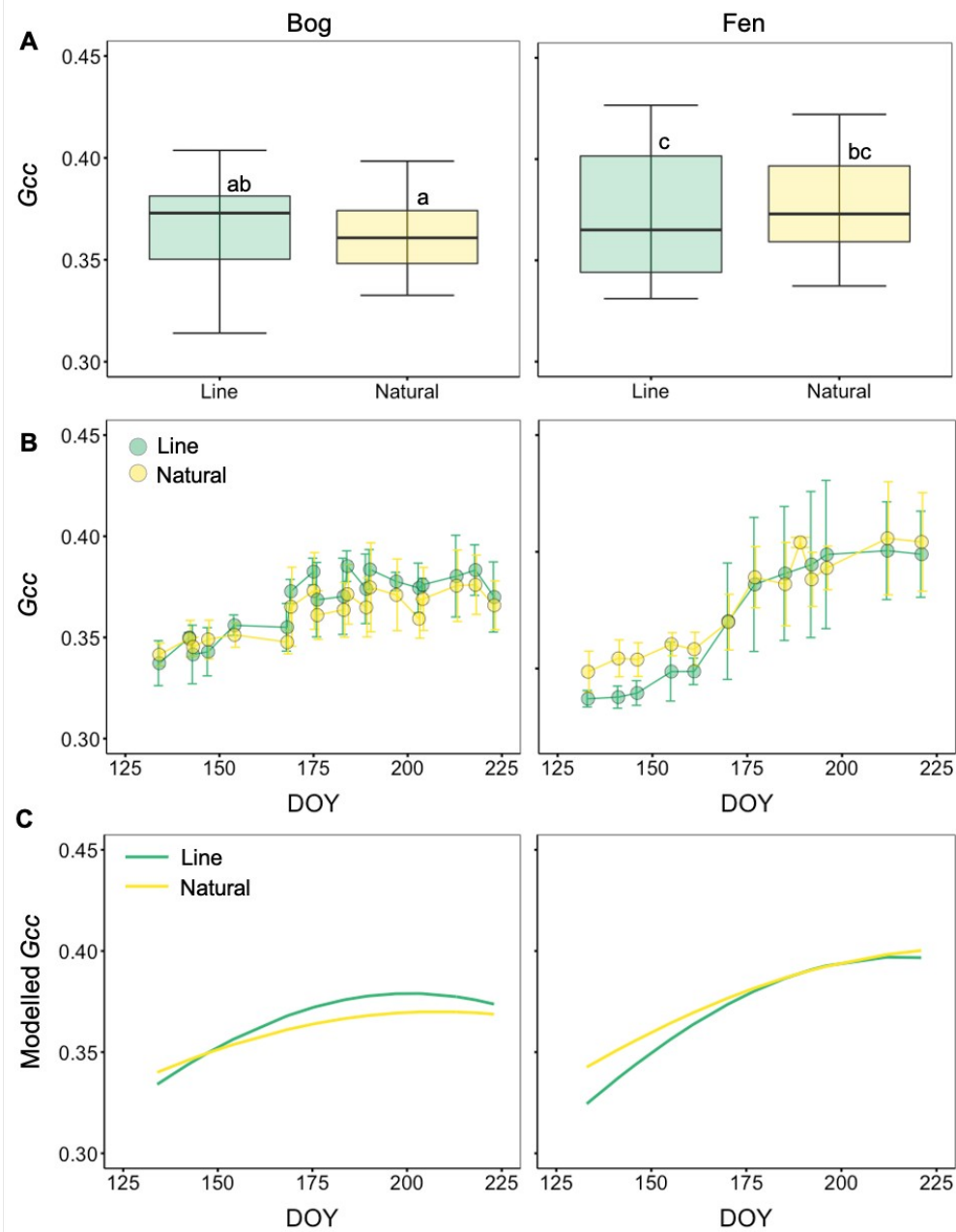254 fen, the seasonal peak of *Gcc* was 19 days earlier than that in natural areas (Table 1).

255

Figure 3. a) box plots of *Gcc* (Bog n = 126, Fen n= 78). Two-way ANOVA followed by a Tukey HSD ($p < 0.05$).
Groups sharing letters are not significantly different, b) Time series of mean (± standard deviation) green chromatic
coordinate (*Gcc*) over the growing season at the bog and fen sites and C) Modelled *Gcc* and associated parameters
(Table 1) suggesting that line sites have an earlier seasonal peak than natural sites.

260

Table 1: Summary of model parameters describing seasonal trajectories of *Gcc* across line and natural bog and fen sites. Peak value is the peak *Gcc* or maximum greenness over the growing season. Critical point is the DOY at peak *Gcc* value. Growth rate of the *Gcc* curve against DOY reflects length of greenness season (larger values have wider curves i.e., longer growing seasons).

| | Bog | | | | Fen | | | |
| | Line | | Natural | | Line | | Natural | |
	Estimate	Std Error	Estimate	Std Error	Estimate	Std Error	Estimate	Std Error
Peak Value	0.38	0.01	0.37	0.00	0.40	0.01	0.40	0.01
Critical Point	201	2.99	208	7.25	215	8.48	234	24.06
Growth Rate	132.80	9.19	180.40	23.52	129.40	15.13	179.54	39.68

261

262   A difference in *Rcc* was also found at both the bog and fen sites between the line and the
263 natural sites, although the effect of disturbance was different between the peatland types. At the
264 bog site, the plots on the line had significantly higher *Rcc* than the nearby adjacent natural area
265 (Figure 4a and c, ANOVA; $F_{1,403} = 82.0$, $p < 0.001$). This was the opposite to the fen site, where
266 the natural site had significantly higher *Rcc* than the plots on the line. Furthermore, at both the
267 disturbed and natural fen sites, the *Rcc* remained stable throughout much of the growing season
268 apart from one time point at the disturbed site (~ day 180) and increasing towards the end of the
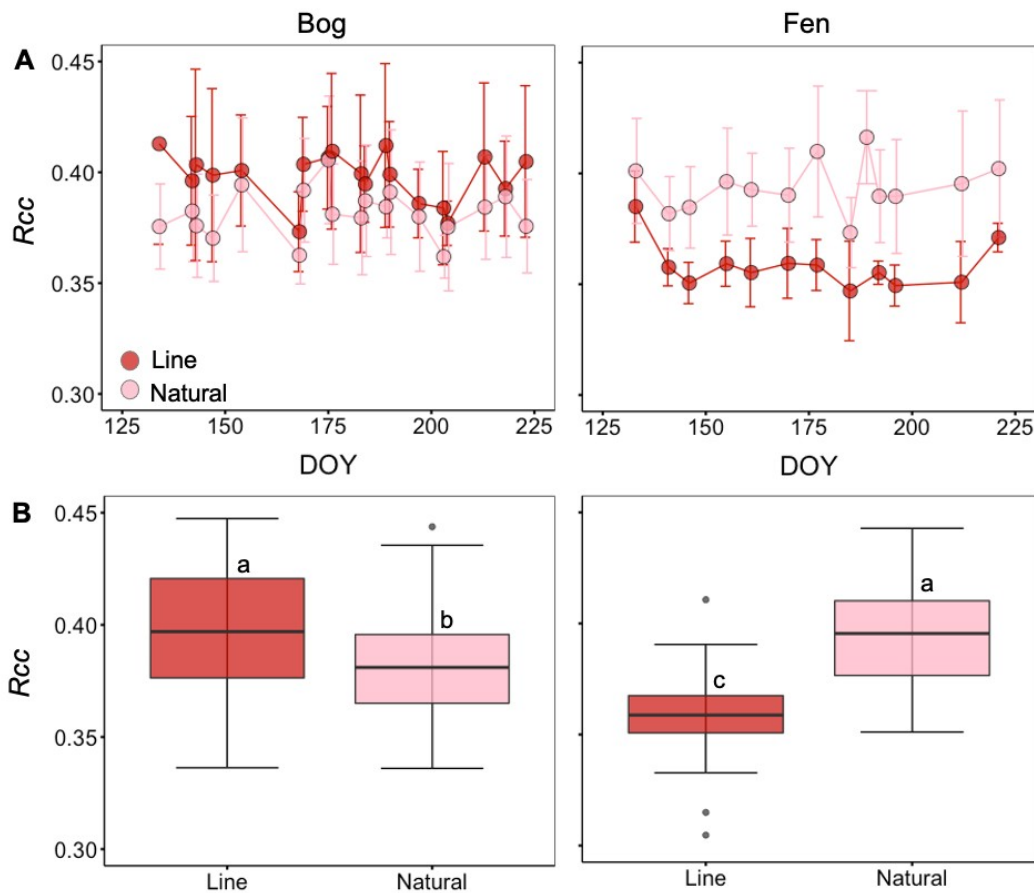269 summer, indicating the beginning of the senescence period.

270
271 **Figure 4**. a) Time series of mean (± standard deviation) red chromatic coordinate (*Rcc*) over the growing season at
272 the bog and the fen sites and b) box plots of *Rcc* (Bog n = 126, Fen n = 78). Two-way ANOVA followed by a Tukey
273 HSD ($p < 0.05$). Groups sharing letters are not significantly different.

274 *3.2 Plant species composition*

275   Sites were primarily distributed along two CA axes that both distinguished between the
276 bog and fen and between natural and disturbed (line) sites (Figure 5a). The first CA axis (27%)
277 distinguished between bog and fen plant communities, and was primarily associated with
278 variation in *Carex aquatilis* Wahlenb*., Cladina rangiferina* (L.) Nyl., and *Salix planifolia* Pursh,
279 with additional contributions from *Sphagnum fuscum* (Schimp.) Klinggr., *Vaccinium oxycoccos*
280 L., and *Vaccinium vitis-idaea* L. The second CA axis (21%) distinguished between natural and
281 line sites across both bog and fen, and was primarily associated with variation in *Pleurozium*
282 *schreberi* (Brid.) Mitt., *Andromeda polifolia* L*., Chamaedaphne calyculata* (L.) Moench, and
283 *Picea mariana* (Mill.) Britton, Sterns & Poggenb., with additional contributions from
284 *Polytrichum strictum* (Brid.), *Rubus chamaemorus* L., and *Cladonia chlorophaea* (Flörke ex
285 Sommerf.) Spreng. *Maianthemum trifolium* (L.) Sloboda, *Rhododendron groenlandicum* (Oeder)
286 K.A. Kron & W.S. Judd, and *Vaccinium cespitosum* Michx. Contributed equally to both CA axes
287 (Table 2). Maximum *Gcc* positively correlated with the first CA axis ($R^2 = 0.23$, p = 0.002;
288 Figure 5b), corresponding to changes in species composition between natural and disturbed (line)

289 sites across bogs and fens (Figure 5b). Maximum *Rcc* was not significantly correlated with the
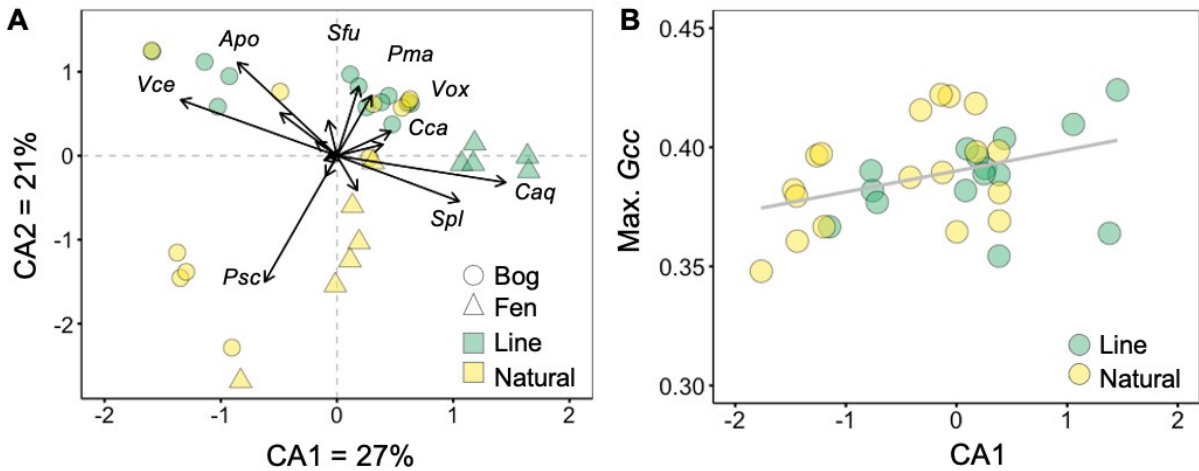290 first CA axis ($R^2 = 0.1$, p = 0.06; Figure S3).

291

292 **Figure 5.** A) Correspondence analysis (CA) plot showing the distribution of natural and disturbed peatland sites in
293 relation to 16 plant species, and B) the relationship between maximum greenness (*Gcc*) and the first CA axis ($R^2 =$
294 0.23, p = 0.002). Species names and abbreviations are found in Table 2.
295

Table 2: Eigenvector loadings for the first two correspondence analysis (CA) axes, describing the strength of associations between the distribution of 16 peatland plant species among natural bog and fen sites, and those disturbed by linear seismic lines.

Species	Abbreviation	CA1	CA2
Andromeda polifolia	Apo	-0.85719	1.11217
Carex aquatilis	Caq	1.45048	-0.31865
Chamaedaphne calyculata	Cca	0.18607	0.82738
Cladina rangiferina	Cra	-1.34465	0.6652
Cladonia chlorophaea	Cch	-0.0742	0.41958
Maianthemum trifolium	Mtr	-0.07206	-0.0185
Picea mariana	Pma	0.29672	0.71567
Pleurozium schreberi	Psc	-0.62162	-1.50083
Polytrichum strictum	Pst	0.1731	-0.41218
Rhododendron groenlandicum	Rgr	-0.18219	0.16921
Rubus chamaemorus	Rch	-0.09649	-0.24086
Salix planifolia	Spl	1.05086	-0.5413
Sphagnum fuscum	Sfu	0.46354	0.2926
Vaccinium cespitosum	Vce	-0.48988	0.50987
Vaccinium oxycoccos	Vox	0.39465	0.13528
Vaccinium vitis-idaea	Vvi	-0.11018	-0.05213

296

297

298   *3.3 Gcc as a predictor of GPP*

299   As hypothesized, we found that *Gcc* was a good predictor of GPP and this relationship
300   differed between natural and disturbed sites. At both the bog and fen, there was a significant
301   interaction between *Gcc* and location (natural vs. line) on GPP (bog; ANCOVA, $F_{1,185}$ = 8.01, p =
302   0.005 and fen; ANCOVA, $F_{1,116}$ = 5.2, p = 0.02) (Figure 6). This arose due to GPP increasing
303   more quickly as *Gcc* increased on lines in natural plots. Overall, there was a significant effect of
304   *Gcc* (ANCOVA, $F_{1,185}$ = 76.7, p < 0.001) and location (natural vs. line) (ANCOVA, $F_{1,185}$ = 53.2,
305   p < 0.001) on GPP at the bog site. This model explained 45% of the variability in GPP.
306   Similarly, at the fen site, there was a significant effect of *Gcc* (ANCOVA, $F_{1,116}$ = 45.4, p <
307   0.001) and location (ANCOVA, $F_{1,116}$ = 74.9, p < 0.001). This model explained 48% of the
308   variability in GPP. Since the rate of change in GPP in response to *Gcc* varied between natural
309   and disturbed sites, we explored whether including *Rcc* in models with *Gcc* (but without
310   disturbance category) could improve GPP prediction. A multiple regression model predicting
311   GPP using both *Gcc* and *Rcc* explained 44% ($F_{4,184}$ = 38.39, p < 0.001) and 46% ($F_{4,115}$ = 26.42, p
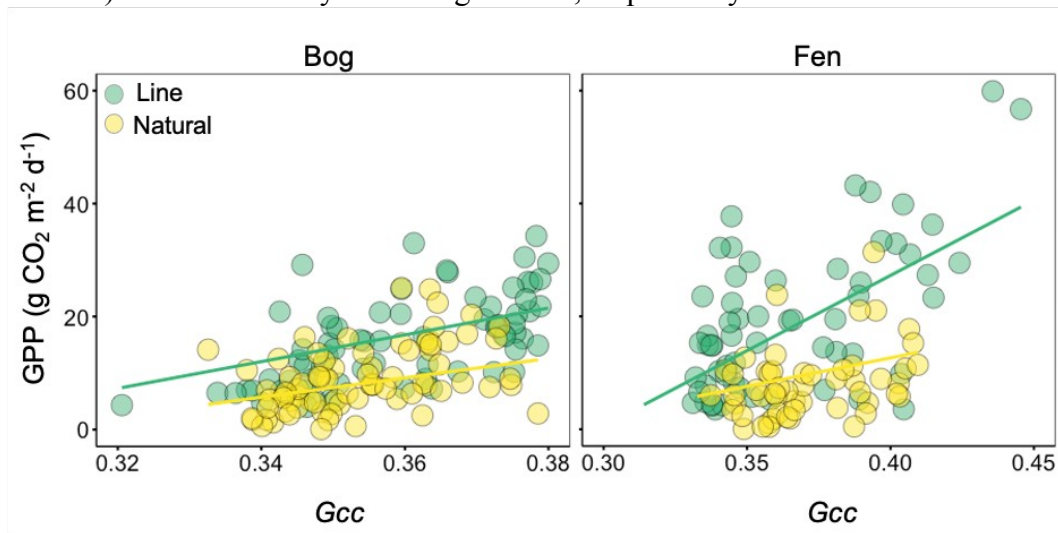312   < 0.001) of the variability at the bog and fen, respectively.

313

314   **Figure 6.** Understory gross primary production (GPP; g CO_2 m^2 d^{-1}) as a function of greenness (green chromatic
315   coordinate; *Gcc*) at both the bog and fen.

316

4. Discussion

318   Our goal was to investigate if linear disturbances from seismic lines impact boreal
319   peatland plant communities and their green leaf phenology, and ultimately the ecosystem carbon
320   function. Our RGB image-based methodology successfully described the seasonal trajectory of
321   plot-level phenology metrics (*Gcc* and *Rcc*) across two different peatland types; thus highlighting
322   a non-destructive and relatively low-cost and low-effort field method for evaluating phenological
323   changes in disturbed peatlands. Our results suggest that seismic lines lead to peatland
324   disturbances wherein a shift in plant species composition alters the phenological trajectory and
325   plot-scale *Gcc* and *Rcc*. Finally, given that our phenological metrics were a strong predictor of
326   CO_2 uptake in our plots, in the future, they could be developed as carbon cycle proxies for rapid
327   disturbance assessments of larger peatland areas.

4.1 Linear disturbance effects on plant phenology, species composition, and carbon exchange

Our results highlight a distinct shift in phenology and species composition between natural sites and seismic lines, with an earlier peak in greenness and overall increases in greenness and productivity in seismic line plots. Specifically, the greenness peak of line plots were 1-3 weeks earlier than in natural areas (Figure 3, Table 1). Variation in greenness was related to changes in plant species composition (Figure 5). At both peatland types, a clear shift in vegetation communities was found on plots located on the seismic line compared to the nearby adjacent undisturbed areas. At the bog site, there was a ground layer of feather moss (*P. schreberi*) and lichen (*C. rangiferina)* in the natural plots and these were replaced by a continuous ground layer of *S. fuscum* on the lines (Figure 5a). Vegetation changes were even more apparent in the fen, with a large shift towards sedge and willow dominance with decreases in moss abundance. The larger *Gcc* values found in the line plots at both sites is likely due to reductions in lichen cover, which has naturally low greenness and photosynthetic rates (Harris et al. 2018). Similarly, the earlier peak in *Gcc* in line plots is likely caused by both an increase in herbaceous perennials that display a strong leaf-out in the spring (e.g., *C. aquatilis*, *R. chamaemorus*) in combination with the loss of mosses (e.g., *P. schreberi*) that stay green late into the autumn (Figure S4). The *Rcc* values measured show an inverse relationship to *Gcc*, especially at the fen site (Figure 4). This is likely due to both the higher red pigmentation of the moss species found in the natural sites compared to the greener species found on the line and senescing leaves towards the end of the summer (Moore et al., 2017).

The creation of seismic lines involves tree removal, flattening of localised microtopography, and peat compaction, resulting in wetter conditions (Lovitt et al., 2018). These environmental disturbances are likely to have caused the observed shifts in understory vegetation, allowing for more moisture-loving species to establish and dominate, such as *C. aquatilis* at the fen and *S. fuscum* at the bog. Linked to this shift in vegetation communities is the reduced likelihood for tree sapling regeneration due to potential competition with more productive understory vegetation such as sedges (Filicetti & Nielsen, 2020). Disturbances across peatlands often result in vegetation shifts following, for example, drainage (Strack et al., 2006), fire (Noble et al., 2019), permafrost thaw (Camill et al., 2001) and flooding/re-wetting (Goud et al., 2018; Tuittila et al., 2000). Increased greenness and primary productivity in the line plots at the fen was likely due to a switch from moss to sedge-dominated communities. Sedges are highly productive, often displaying larger rates of growth and carbon exchange relative to lichen, mosses and shrubs (Goud et al. 2017; Harris et al., 2018). Given that a dominance of sedges allows for more CO_2 uptake (Leppälä et al., 2008), this may explain the tighter and steeper relationship between greenness and GPP on seismic lines, particularly at the fen (Figure 6). Although there are relatively few studies on carbon exchange following linear disturbances, Strack et al. (2018) also found a significant increase in graminoid cover on a winter road crossing a boreal peatland. Similar to our results, this linear disturbance impacted hydrology and carbon dynamics, with disturbed plots having greater CO_2 uptake compared to the adjacent peatland. The removal of the tree canopy also reduces overall tree biomass and associated net primary production, further influencing carbon stocks in these systems. In the long term, it is possible that understory productivity could increase enough to compensate for this loss, indicative of a potential tradeoff between overstory and understory carbon uptake following disturbance (Strack et al., 2018). However, the shift towards a more sedge-dominated system at the fen site in this study could not only lead to more carbon uptake but could also lead to higher respiration rates and larger CH_4 emissions through increased rates of plant-mediated transport

374 (Strack et al., 2018). Given that Strack et al. (2019) calculated that there are approximately 790
375 km^2 of seismic lines crossing fens in Alberta alone, potentially leading to a substantial increase
376 in CH$_4$ emissions, this has widespread implications for the carbon balance and net radiative
377 forcing of these systems.
378

379 *4.2 Applications of phenological measurements for peatland monitoring and management*

380   Monitoring phenology is a useful metric for understanding disturbance-induced
381 vegetation shifts and function and could provide a useful way of identifying restoration progress
382 and future priority areas. In this study, using a smartphone to collect imagery eliminated the need
383 for fixed infrastructure, allowing us to sample more small-scale (understory) plots and study sites
384 relative to other commonly used phenological methods such as remote sensing and meaurements
385 of plant anatomical traits and biomass. Although digital photograph collection provides a lower
386 temporal resolution than we would get from a fixed or remote sensing platform, it provides an
387 accessible low-cost method with many advantages (Weil et al. 2017). Hand held digital
388 photography allowed us to focus on the understory peatland vegetation communities, rather than
389 having to use a landscape-scale image which would likely mask any ground-layer changes in
390 vegetation community and phenology. Field-based spectral reflectance discrimination of
391 peatland and tundra vegetation communities have been successfully undertaken in various
392 studies (Bubier et al., 1997; Davidson et al., 2016). Similar methodologies could be applied
393 using phenological data. The significant differences in the chromatic coordinates, in particular
394 the *Rcc,* between disturbed and natural plots indicate its usefulness as a tool for monitoring
395 differences in species composition following disturbance at larger spatial scales without needing
396 to go further and use more expensive near infra-red based sensors (Weil et al., 2017). This could
397 prove especially useful in terms of peatland restoration and when trying to understand poor tree
398 recovery on seismic lines through competition with other peatland plant species such as
399 *Sphagnum* or sedge species. Furthermore, our ability to link the easy-to-measure *Gcc* and *Rcc*
400 with GPP also shows promise as a way to monitor and map shifts in peatland carbon exchange in
401 response to linear disturbances and recovery over time. This would be valuable to regional to
402 national accounting of greenhouse gas emissions. Finally, the greenness measured at the plot
403 scale using these photographs could be upscaled using remote sensing products (e.g. high
404 resolution, high frequency satellite imagery such as Planet (PlanetLabs, San Francisco, USA)
405 that incorporate the overstory canopy in order to investigate temporal changes in vegetation
406 productivity across much larger spatial scales and help improve management and restoration
407 post-disturbance.
408

5. Conclusion

410   Peatlands across the boreal zone in Canada and their vast carbon stocks are vulnerable to
411 climate and land-use change. Vegetation communities and their phenological trajectory are often
412 the first ecosystem components to respond to environmental change and may influence peatland
413 net carbon balance. Here, we demonstrate a low-cost and readily available method to assess
414 phenological change in peatlands. We observe strong phenological changes in peatlands
415 disturbed by seismic lines and find that these changes are driven by vegetation community shifts,
416 and ultimately, influence ecosystem carbon uptake. We provide an easy-to-use method that
417 could help improve the understanding of vegetation community, phenology and carbon exchange

418 post-disturbance across a variety of different ecosystems with high spatial resolution without the
419 need for fixed infrastructure and expensive sensors. Since boreal landscapes will continue to be
420 threatened by a variety of disturbances, improving our understanding of the magnitude and
421 mechanisms of vegetation and phenology changes post-disturbance is the first step toward
422 predicting changes to the carbon cycle of these ecosystems across broad spatial scales.
423

CRediT author statement

Scott J. Davidson: Conceptualization, Methodology, Formal analysis, Investigation, Writing –
Original Draft and Review & Editing, Visualization, Project administration **Ellie M. Goud:**
Formal analysis, Writing – Review & Editing **Avni Malhotra:** Formal analysis, Writing –
Review & Editing **Claire O Estey:** Investigation, Writing – Review & Editing **Percy Korsah:**
Conceptualization, Writing – Review & Editing **Maria Strack:** Conceptualization, Writing –
Review & Editing, Superivision, Funding acquisition.

Declaration of Interest

The authors declare that they have no known competing financial interests or personal
relationships that could have appeared to influence the work reported in this paper

Data availability statement

Data available via the Dryad Digital Repository:
Davidson, Scott (2021), Davidson_boreal_peatland_phenology,
https://doi.org/10.5061/dryad.x69p8czhh

Acknowledgements

References

455   Alm, J., Shurpali, N., Tuittila, E.-S., Laurila, T., Maljanen, M., Saarnio, S. & Minkkinen, K.
456   (2007). Methods for determining emission factors for the use of peat and peatlands; flux
457   measurements and modelling. *Boreal Environment Research*, 12, 85–100.
458   Brandt, J.P. (2009). The extent of the North American boreal zone. *Environmental Reviews*,
459   17:101–161
460   Bubier, J.L., Barrett, N.R. & Krill, P.M. (1997). Spectral Reflectance Measurements of Boreal
461   Wetland and Forest Mosses, *Journal of Geophysical Research: Atmospheres*
462   https://doi.org/10.1029/97jd02316
463   Bubier, J.L., Moore, T.R. & Crosby, G. (2006). Fine-scale vegetation distribution in a cool
464   temperate peatland. *Canadian Journal of Botany,* 84 (6): 910-923
465   Camill, P., Lynch, J.A., Clark, J.S., Adams, J.B. & Jordan, B. (2001). Changes in Biomass,
466   Aboveground Net Primary Production, and Peat Accumulation following Permafrost
467   Thaw in the Boreal Peatlands of Manitoba, Canada. *Ecosystems*, 4: 461-478
468   Dabros, A., Pyper, M. & Castilla, G. (2018). Seismic lines in the Boreal and Arctic Ecosystems
469   of North America: Environmental Impacts, Challenges and Opportunities. *Environmental
470   Review*, 26 (2): 214-229
471   Davidson, S.J., Goud, E.M., Franklin, C., Nielsen, S.E. & Strack, M. (2020). Seismic line
472   Disturbance Alters Soil Physical and Chemical Properties Across Boreal Forest and
473   Peatland Soils. *Frontiers in Earth Science*. https://doi.org/10.3389/feart.2020.00281
474   Davidson, S.J., Santos, M.J., Sloan, V.L., Watts, J., Phoenix, G.K., Oechel, W.O. & Zona, D.
475   (2016). Mapping Arctic Tundra Vegetation Communities Using Field Spectroscopy and
476   Multispectral Satellite Data in North Alaska, USA. *Remote Sensing* 8 (12): 978
477   Echiverri, L.F.I., Macdonald, S.E. & Nielsen, S.E. (2020). Disturbing to restore? Effects of
478   mounding on understory communities on seismic lines in treed peatlands. *Can. J. For.
479   Res*. 50: 1340-1351
480   Filicetti, A.T., Cody, M. & Nielsen, S.E. (2019). Caribou Conservation: Restoring Trees on
481   Seismic   lines,   Alberta,   Canada.   *Remote   Sensing*,   10(2),
482   185; https://doi.org/10.3390/f10020185
483   Filicetti, A.T. & Nielsen, S.E. (2020). Tree regeneration on industrial linear disturbances in treed
484   peatlands is hastened by wildfire and delayed by loss of microtopgraphy. *Can. J. For.
485   Res*. 50, 936-945.
486   Filippa, G., Cremonese, E., Migliavacca, M., Galvagano, M., Forkel, M., Wingate, L., Tomelleri,
487   E., Morra di Cella, M. & Richardson, A.D. (2016). Phenopix: a R Package for Image-
488   Based   Vegetation   Phenology.   *Agricultural   and   Forest   Meteorology*,
489   https://doi.org/10.1016/j.agrformet.2016.01.006

490   Girard, A., Schweiger, A.K., Carteron, A., Kalacsk & M, Laliberté, E. (2020). Foliar Spectra and
491   Traits of Bog Plants across Nitrogen Deposition Gradients. *Remote Sensing*. 12 (15):
492   2448
493   Goud, E.M., Moore, T.R. & Roulet, N.T. (2017). Predicting Peatland Carbon Fluxes from Non-
494   destructive Plant Traits. *Functional Ecology*, https://doi.org/10.1111/1365-2435.12891
495   Goud, E.M., Watt, C. & Moore, T.R. (2018). Plant community composition along a peatland
496   margin follows alternate successional pathways after hydrologic disturbance. *Acta
497   Oecologica*. doi: 10.1016/j.actao.2018.06.006
498   Hanson P.J., Griffiths, N.A., Iversen, C.M., Norby, R.J., Sebestyen, S.D., Phillips, J.R., Chanton,
499   J.P., Kolka, R.K., Malhotra, A., Oleheiser, K.C., Warren, J.M., Shi, X., Yang, X., Mao, J.
500   & Ricciuto, D.M. (2020). Rapid Net Carbon Loss From A Whole-Ecosystem Warmed
501   Peatland. *AGU Advances*, 1, e2020AV000163
502   Harris, L.I., Moore, T.R., Roulet, N.T. & Pinsonneault, A.J. (2018). Lichens: A limit to peat
503   growth? *Journal of Ecology*. 106 (6), 2301-2319.
504   Hufkens, K., Friedl, M., Sonnentag, O., Braswell, B.H., Milliman, T. & Richardson, A.D.
505   (2012). Linking near-Surface and Satellite Remote Sensing Measurements of Deciduous
506   Broadleaf Forest Phenology. *Remote Sensing of Environment*,
507   https://doi.org/10.1016/j.rse.2011.10.006
508   Korrensalo, A., Mannisto, E., Alekseychik, P., Mammarella, I., Rinne, J., Vesala, T. & Tuittila,
509   E.-S. (2018). Small Spatial Variability in Methane Emission Measured from a Wet
510   Patterned Boreal bog. *Biogeosciences*, 15 (6): 1749-1761
511   Lavorel, S. & Garnier, E. (2002). Predicting changes in community composition and ecosystem
512   functioning from plant traits: revisiting the Holy Grail. *Functional Ecology*, 16, 545–556
513   Legendre, P. & Legendre, L. (2012). Numerical ecology eds. Legendre, P, Legendre, L
514   (Elsevier). 3rd Ed.
515   Leppälä, M., Kukko-Oja, K., Laine, J. & Tuittila, E.-S. (2008). Seasonal dynamics of CO_2
516   exchange during primary succession of boreal mires as controlled by phenology of plants.
517   *Écoscience*, 15 (4): 460-471.
518   Linkosalmi, M., Aurela, M., Tuovinen, J-P., Peltoniemi, M., Tanis, C.M., Arslan, A.N., Kolari,
519   P., Böttcher, K., Aalto, T., Rainne, J., Hatakka, J. & Laurila, T. (2016). Digital
520   photography for assessing the link between vegetation phenology and CO_2 exchange in
521   two contrasting northern ecosystems. *Geosci. Intrsum. Method. Data. Sci*. 5, 417-426.
522   Liu, U., Wu, C., Sonnentag, O., Desai, A.R. & Wang, J. (2020). Using the Red Chromatic
523   Coordinate to Characterize the Phenology of Forest Canopy Photosynthesis. *Agricultural
524   and Forest Meteorology*. https://doi.org/10.1016/j.agrformet.2020.107910
525   Lovitt, J., Rahman, M.M., Saraswati, S., McDermid, G.J., Strack, M. & Xu, B. (2018). UAV
526   Remote Sensing Can Reveal the Effects of Low-Impact Seismic lines on Surface
527   Morphology, Hydrology and Methane (CH_4) Release in a Boreal Treed bog. *Journal of
528   Geophysical Research: Biogeosciences*, 123 (3): 1117-1129
529   Malhotra, A. & Roulet, N.T. (2015). Environmental correlates of peatland carbon fluxes in a
530   thawing landscape: do transitional thaw stages matter. *Biogeosciences*. 12, 3119-3130
531   Malhotra, A., Brice, D., Childs, J., Graham, J.D., Hobbie, E.A., Vander Stel, H., Feronm S.C.,
532   Hanson, P.J. & Iversen, C.M. (2020). Peatland warming strongly increases fine-root
533   growth. *PNAS*.117:30, 17627-1763410
534   Moore, C.E., Beringer, J., Evans, B., Hutley, L.B. & Tapper, N.J. (2017). Tree-grass phenology
535   information improves light use efficiency modelling of gross primary productivity for an

Australian tropical savanna. *Biogeosciences*, 14, 111-129.

Noble, A., Palmer, S.M., Glaves, D.J., Crowle, A. & Holden, J. (2019). Peatland vegetation change and establishment of re-introduced *Sphagnum* moss after prescribed burning. *Biodiversity and Conservation.* 28: 939-952.

Oksanen, J, Blanchet, F.G., Friendly, M., Kindt, R., Simpson, G.L., Legendre, P., McGlinn, D., Minchin, P.R., O'Hara, R.B., Solymos, P., Stevens, M.H.H., Szoecs, E. & Wagner, H. (2019). Vegan: Community Ecology Package, Version 2.5.-6. https://rdrr.io/cran/vegan/

Peichl, M., Sonnentag, O. & Nilsson, M.B. (2015). Bringing Color into the Picture: Using Digital Repeat Photography to Investigate Phenology Controls of the Carbon Dioxide Exchange in a Boreal Mire. *Ecosystems*. https://doi.org/10.1007/s10021-014-9815-z

Pyper, M., Nishi, J. & McNeil, L. (2014). Linear feature restoration in caribou habitat: a summary of current practices and a roadmap for future programs. Prepared for Canada's Oil Sands Innovation Alliance, Edmonton, Alberta.

R Core Team. 2019. R: A language and environment for statistical computing (Vienna, Austria) Available at: https://www.R-project.org/.

Richardson, A.D., Hufkens, K., Milliman, T., Aubrecht, D.M., Furze, M.E., Seyednasrollah, B., Krassovski, M.B., Latimer, J.M., Nettles, W.R., Heiderman, R.R., Warren, J.M. & Hanson, P.J. (2018). Ecosystem warming extends vegetation activity but heightens vulnerability to cold temperatures. *Nature*, 560 (7718), 368–371. https://doi.org/10.1038/s41586-018-0399-1

Robroek, B.J.M., Jassey, V.E.J., Payne, R.J., Marti, M., Bragazza, L., Bleeker, A., Buttler, A., Caporn, S.J.M., Dise, N.B., Kattge, J., Zając, K., Svensson, B.H., van Ruijven, J. & Verhoeven, J.T.A. (2017). Taxonomic and functional turnover are decoupled in European peat bogs. *Nature Communications*, 8:1161.

Sonnentag, O., Hufkens, K., Teshera-Sterne, C., Young, A.M., Friedl, M., Braswell, B.H., Milliman, T., O'Keefe, J. & Richardson, A.D. (2012). Digital Repeat Photography for Phenological Research in Forest Ecosystems. *Agricultural and Forest Meteorology*. https://doi.org/10.1016/j.agrformet.2011.09.009

Strack, M., Hayne, S., Lovitt, J., McDermid, G.J., Rahman, M.M., Saraswati, S. & Xu, B. (2019). Petroleum exploration increases methane emissions from northern peatlands. *Nature Communications*. 10:2804 | https://doi.org/10.1038/s41467-019-10762-4

Strack, M., Softa, D., Bird, M. & Xu, B. (2018). Impact of winter roads on boreal peatland carbon exchange. *Global Change Biology*, 24:e201–e212.

Strack, M., Waller, M.F. & Waddington, J.M. (2006). Sedge succession and Peatland Methane Dynamics: A Potential Feedback to Climate Change. *Ecosystems*, 9, 278-287.

Toomey, M., Friedl, M.A., Frolking, S., Hufkens, K., Klosterman, S., Sonnentag, O., Baldocchi, D.D., Barnacchi, C.K., Biraud, S.C., Bohrer, G., Brozstek, E., Burns, S.P., Coursolle, C., Hollinger, D.Y., Margolis, H.A., McCaughey, H., Monsoon, R.K., Munger, J.W., Pallardy, S., Phillips, R.P., Torn, M.S., Wharton, A., Zeri, M. & Richardson, A.D. (2015). Greenness indices from digital cameras predict the timing and seasonal dynamics of canopy-scale photosynthesis. *Ecological Applications*, 25 (1): 99-115

Tuittila, E.-S., Vasander, H. & Laine, J. (2000). Impact of rewetting on the vegetation of a cut-away peatland. *Applied Vegetation Science*, 3: 205-212.

Weil, G., Lensky, I.M. & Levin, N. (2017). Using ground observations of a digital camera in the VIS-NIR range for quantifying the phenology of Mediterranean woody species. *Int. J. Appl. Earth. Obs. Geoinformation*. 62, 88-101.

White, M.A., Thornton, P.E. & Running, S.W. (1997). A continental phenology model for monitoring vegetation response to interannual climatic variability. *Global Biogeochemical Cycles*, 11 (2), 217-234. https://doi.org/10.1007/s11258-006-9189-1

Wieder, R.K., Vitt, D.H. & Benscoter, B.W. (2006). Peatlands and the Boreal forest. In: *Boreal Peatland Ecosystems*, Ecological Studies 188 (eds Wieder RK, Vitt DH), pp. 1-8. Springer-Verlag, Heidelberg, Germany.

Wilson, D., Alm, J., Riutta, T., Laine, J., Byrne, K.A., Farrell, E.P. & Tuittila, E.-S. (2007). A High-Resolution Green Area Index for Modelling the Seasonal Dynamics of CO_2 Exchange in Peatland Vascular Plant Communities. *Plant Ecology*. 190, 37–51.

Wu, N., Shi, R., Zhuo, W., Zhang, X., Zhou, B., Xia, Z., Tao, Z., Gao, W. & Tian, B. (2021). A Classification of Tidal Flat Wetland Vegetation Combining Phenological Features with Google Earth Engine. *Remote Sensing*, 13, 443. https://doi.org/10.3390/rs13030443

Zeh, L., Igel, M.T., Schellekens, J., Limpens, J., Bragazza, L. & Kalbitz, K. (2020). Vascular plants affect properties and decomposition of moss-dominated peat, particularly at elevated temperatures. *Biogeosciences*, 17: 4797-4813